Effect of Controlled Shot Peening and Laser Shock Peening on the Fatigue Performance of 2024-T351 Aluminum Alloy

C.A. Rodopoulos, J.S. Romero, S.A. Curtis, E.R. de los Rios, and P. Peyre

(Submitted 3 December 2002; in revised form 20 February 2003)

The influence of shot peening, laser shock peening, and dual (shot and laser peening) treatment on the fatigue behavior of 2024-T351 was investigated. Tests showed a fatigue life improvement in all three cases with laser shock peening and dual treatment displaying fatigue performance superior to shot peening. Fractographic analysis showed that the relatively poor performance of the shot peening is caused by ductility loss.

Keywords 2024-T351, dual treatment, four-point fatigue testing, laser shock peening, shot peening

1. Introduction

The potential of using surface engineering techniques, such as controlled shot peening (CSP) and laser shock peening (LSP), to improve the fatigue resistance of monolithic materials has long been recognized by the automotive and the aerospace industries.[1] The beneficial effect brought about by CSP and LSP derives mainly from the generation of a stable compressive residual stress profile and strain hardening in the near surface region.[2] Compressive residual stresses are the more important of the two in the case of high strength materials. However, in softer materials strain hardening dominates, since partial or complete relaxation of the residual stresses may occur.[3] Strain hardening has been reported to decelerate microcrack growth but to accelerate long crack propagation due to low residual ductility.[4,5] In high strength materials, however, the beneficial effect of the compressive residual stress can be compromised by the development of subsurface cracking, usually in the regions where tensile residual stress balances the compressive residual stress field.[6] Subsurface cracking may even be detrimental in smooth fatigue specimens or in components where surface initiation is not considered to be the critical nucleation site.[7,8] Roughening of the surface is the major detrimental effect of CSP. Surface roughness due to the local intensification of the far-field stress can account for the premature initiation and propagation of short fatigue cracks.[9]

The latter indicates that the application of surface engineering to improve fatigue resistance is not straightforward and that there may be cases where surface engineering can even have the opposite effect. To establish with certainty the conditions under which CSP and LSP would produce beneficial results, an investigation of these surface treatments in terms of the fatigue resistance of 2024-T351 aluminum alloy was undertaken.

C.A. Rodopoulos, J.S. Romero, S.A. Curtis, and **E.R. de los Rios,** Division of Aeronautical Applications, Department of Mechanical Engineering, The University of Sheffield, Sheffield, S1 3JD, UK; and **P. Peyre,** CLFA-LALP, 94114 Arcueil, France. Contact e-mail: c.rodopoulos@sheffield.ac.uk.

2. Shot and Laser Shock Peening Conditions

Material, supplied by Airbus UK (Filton, UK), was received in the form of a 30.0 mm thick rolled plate. A full chemical composition and the mechanical properties are given in Tables 1 and 2, respectively. The material has a pancake-shaped grain structure with an average grain size of $220 \times 80 \times 52$ μm in the longitudinal, transverse, and thickness directions.

Controlled shot peening was performed using a Tealgate (Tealgate, Cambridge, UK) peening machine. The peening intensity was 4A and it was achieved using a S110 (diameter 0.279 mm and hardness 410.5–548.5 Hv) spherical cast steel shot, incidence angle of 45°, and a coverage rate of 200%. These conditions were recommended in Ref. 12 in which a study of maximum, near surface, residual stress profile to counterbalance the increased surface roughness profile was made. These residual stress and strain hardening distributions are shown in Fig. 1. The results indicate that the selected CSP conditions deliver a generous strain hardening in the 0-100 μm region.

Laser shock peening was performed in water confinement using a Continuum YAG Laser (Powerlite plus) operating in the green wavelength (0.532 μm) range. The output energy was approximately 1.3 J with pulse duration in the 6-7 ns range. All specimens were protected from the thermal effects of LSP by a 70 μm aluminum coating. The laser intensity was set to 10GW/cm^2 (estimated pressure of 5 GPa) with a focal point of 2 mm. The specimens were treated using an overlapping rate of 50% (1 pass = 4 local pulses) and charged with 2-3 passes. Residual stress and microhardness distribution are shown in Fig. 2. Microhardness results for both LSP conditions indicate negligible strain hardening.

Table 1 Chemical Composition of 2024-T351 in wt.%[10]

Si	Fe	Cu	Mn	Mg	Cr	Zn	Ti	Al
0.05	0.5	3.8-4.9	0.3-0.9	1.2-1.8	0.1	0.25	0.15	Bal.

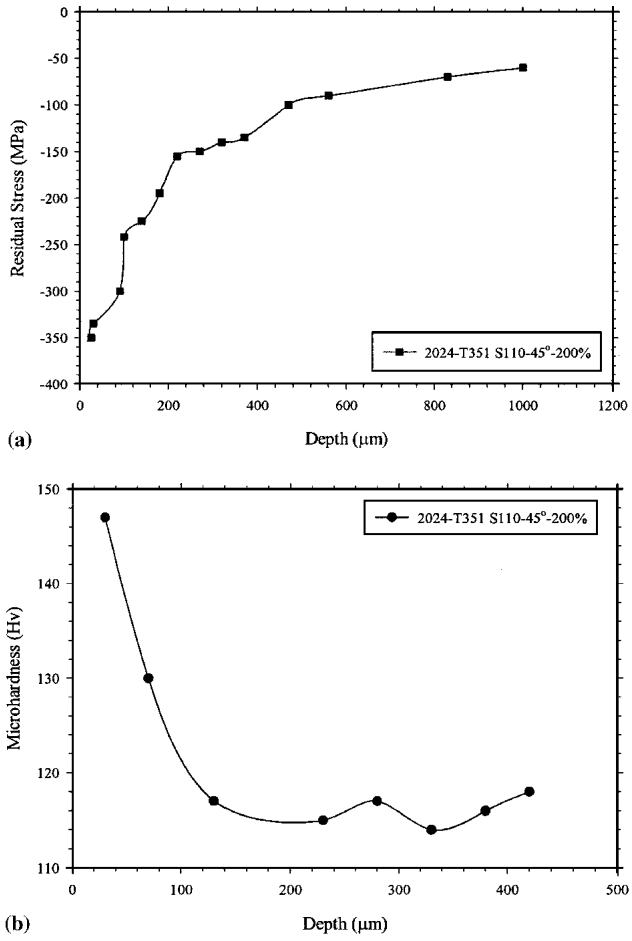

Fig. 1 **(a)** Residual stress distribution for 2024-T351 peened to a 4A intensity. The obtained measurements were in accordance to ASTM E837-95 (hole-drilling) standard. **(b)** Microhardness distribution for 2024-T351 peened to 4A intensity

Table 2 Mechanical and Physical Properties of 2024-T351 at Room Temperature[10,11]

Elastic Modulus, GPa	72.4	Hardness, HB	115-120
Shear Modulus, GPa	27.21	P. Strain Toughness, $MPam^{1/2}$	34
Poisson's Ratio	0.33	Ult. Tensile Strength, MPa	470-520
Mon. Yield Stress, MPa	325-340	Fatigue Limit, R = −1	135-140
Cyclic Yield Stress, MPa	420-450	Shear Strength, MPa	285
Melting Temperature, °C	660-700		
Density, g/cm^3	2.77		

To investigate the possibility of improving the residual stress profile by pre-stressing, a 4A intensity CSP treatment was introduced prior to LSP. The resulting residual stress profile is shown in Fig. 3.

Figure 3 indicates that the dual treatment has a better residual stress distribution than the single CSP or LSP treatments. Even though the profile is strongly influenced by the CSP, the residual stresses are larger and deeper. Microhardness measurements show a similar profile to that of the CSP shown

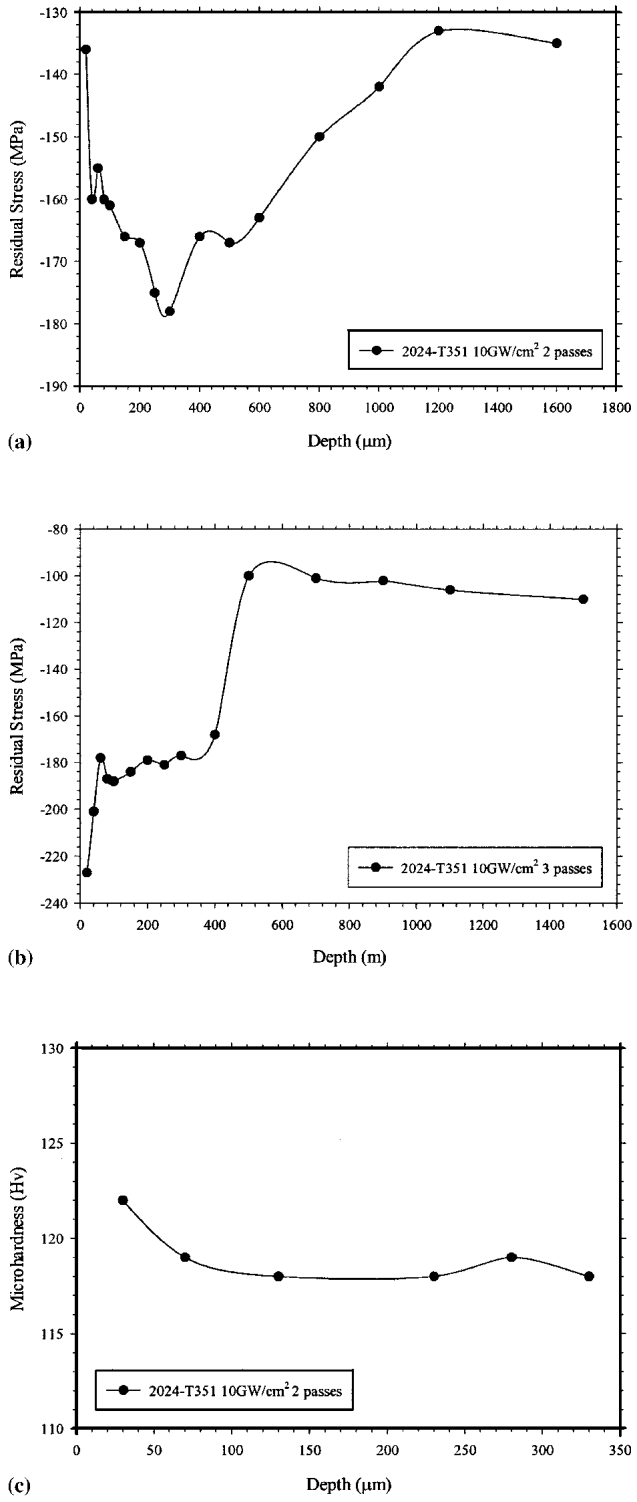

Fig. 2 **(a)** Residual stress distribution for 2024-T351 laser shock peened with a laser intensity of $10GW/cm^2$ and 2 passes. The obtained measurements were in accordance to ASTM E837-95 (hole-drilling) standard. **(b)** Residual stress distribution for 2024-T351 laser shock peened with a laser intensity of $10GW/cm^2$ and 3 passes. The obtained measurements were in accordance to ASTM E837-95 (hole-drilling) standard. **(c)** Microhardness distribution for 2024-T351 laser shock peened with a laser intensity of $10GW/cm^2$ and 2 passes. Results show negligible hardening.

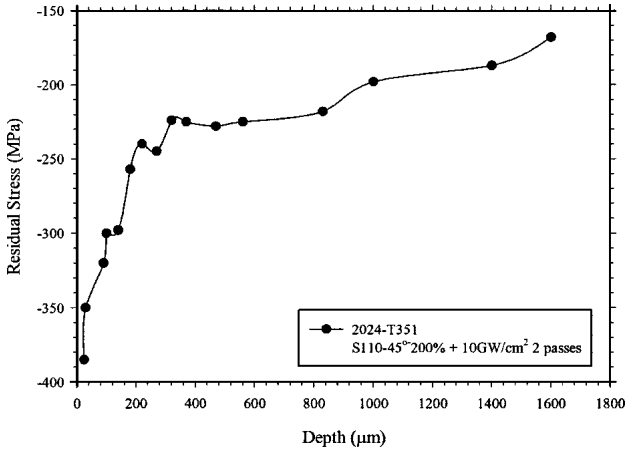

Fig. 3 Residual stress distribution for dual treatment (CSP 4A + LSP 10GW/cm^2 and 2 passes) in 2024-T351. The obtained measurements were in accordance to ASTM E837-95 (hole-drilling) standard.

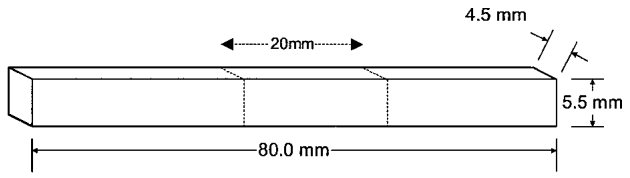

Fig. 4 Test-piece dimensions; the dotted lines represent the gauge area.

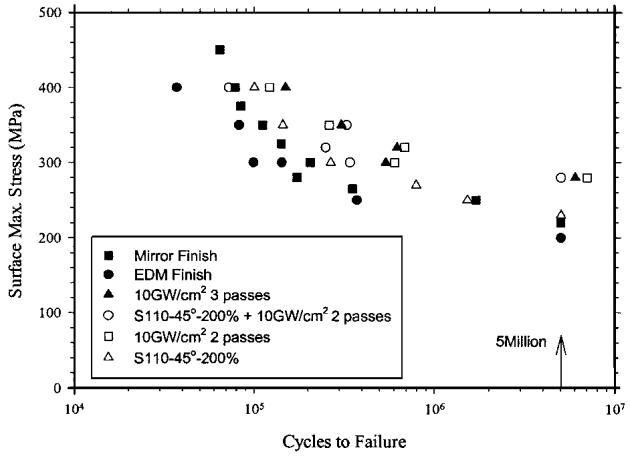

Fig. 5 Average value S-N curves (95% scatter confidence) of the six selected test groups; all data beyond the 5 million cycles mark represent run-outs.

in Fig. 1(b). This verifies once again that LSP in 2024-T351 does not cause strain hardening.

2.1 Fatigue Testing and Results

Fatigue testing was performed with four-point bend loading to investigate the effect of a stress gradient and to minimize the possibility of subsurface cracking. Test pieces were cut parallel to the rolling direction using electro-discharge machining (EDM). Test-piece dimensions are shown in Fig. 4. The stress gradient is given by the linear relationship $\sigma/\sigma_{max} = 0.36z$, where z is the position of the bending fiber from the neutral/central fiber. Six different groups of treatments and surface conditions were selected to investigate the effect of CSP, LSP, combination of CSP and LSP, and initial surface finish on fatigue resistance. Prior to testing, average surface profiles were taken (Table 3) to investigate the effect of CSP, LSP, and CSP + LSP on the original surface roughness. In Table 3, the parameter $R_{a\ is}$ the center-line average, R_t is the maximum peak-to-valley height, and S is the mean spacing of adjacent peaks.

The results shown in Table 3 indicate that LSP does not affect the initial roughness of the target material, except for the 3 passes condition, which showed a slight increase in surface roughness. Conversely, CSP considerably roughened the surface. From Ref. 9, the elastic stress concentration due to CSP surface roughening is given by

$$K_t = 1 + 1.05\,\frac{R_t}{S} \qquad \text{(Eq 1)}$$

Equation 1 takes into account both the uniformity and the root radius of the dents. Using Eq 1 and the corresponding values from Table 3, an elastic stress concentration of $K_t \approx 1.27$ is determined for both the single 4A CSP intensity and the dual treatment.

Fatigue experiments were conducted at room temperature. All tests were performed using a sinusoidal waveform, at a frequency of 15Hz, and a stress ratio (minimum to maximum stress ratio) of $R = 0.1$. Fatigue data in the form of *S/N* curves are shown in Fig. 5.

The results indicate that the two LSPs and the dual treatment can significantly increase the fatigue life of the material independently of their original surface finish. The dual treatment, however, showed an inferior performance compared with the single LSP treatment, which confirms the findings made in Ref. 4 and 5 about low residual ductility. On the other hand, life improvement due to CSP is only realized when compared with the EDM finish. Compared with the mirror finish, CSP

Table 3 Average Surface Roughness Values of Selected Testing Conditions

Roughness Parameters	Mirror Finish (a)	EDM Finish	S110-45°-200%	10GW/cm2 2 Passes	S110-45°-200% + 10 GW/cm2 2 Passes	10 GW/cm2 3 Passes
R_a, μm	0.278	4.015	4.689	4.020	4.689	4.210
R_t, μm	3.310	26.565	30.930	27.903	30.930	34.406
S, mm	0.048	0.073	0.122	0.076	0.122	0.088

(a) The mirror finish was achieved using a succession of finer grade emery papers and diamond pastes to a ¼ micron size.

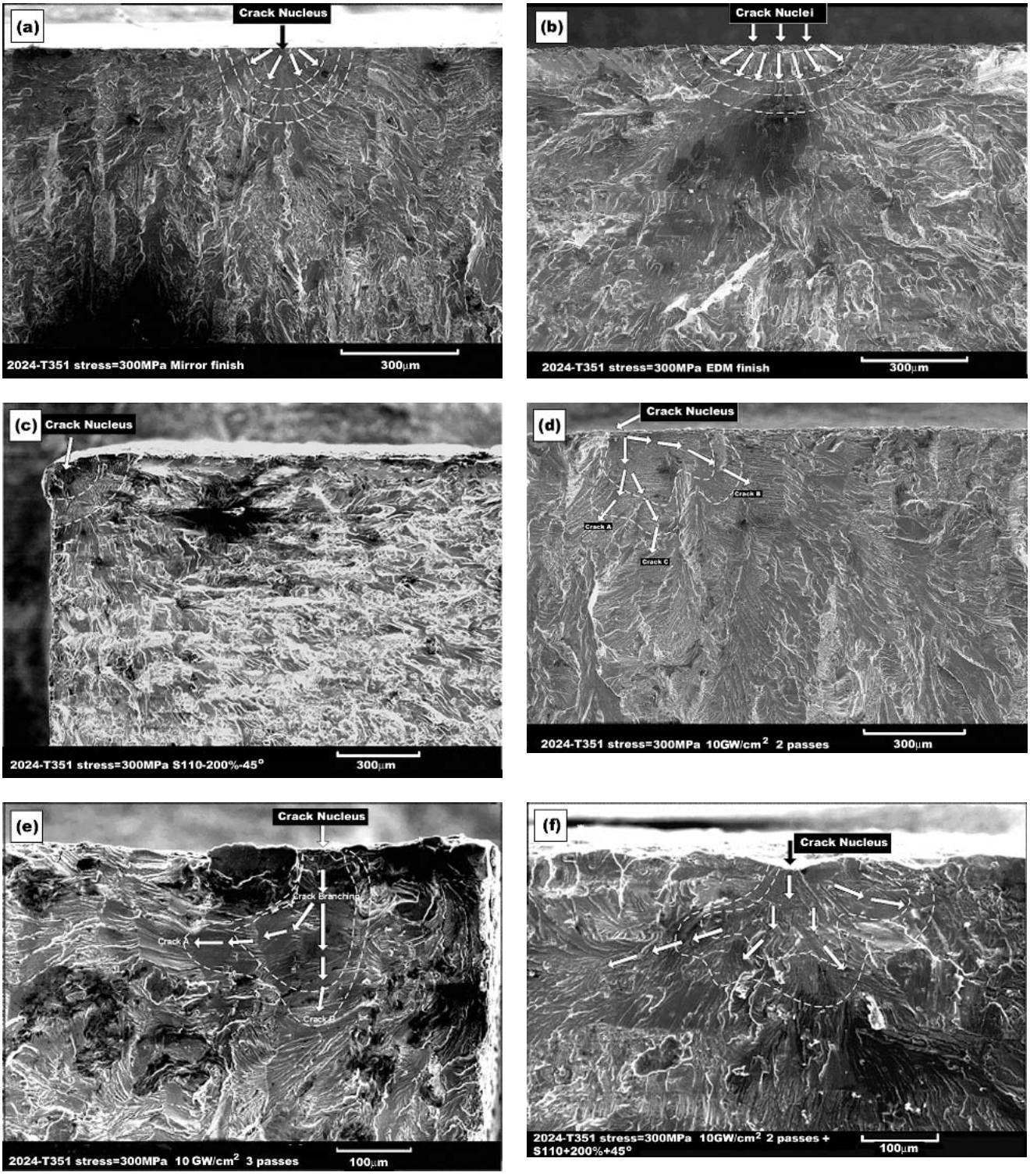

Fig. 6 **(a)** Surface crack initiation and crack growth of pristine material with mirror finish. The fractograph clearly indicates the faceted growth (shear mode growth). **(b)** Surface crack initiation and crack growth of pristine material with EDM finish. The near surface region shows evidence of multiple crack nuclei, possible caused by the irregular surface. **(c)** Site of corner crack initiation and crack growth morphology of an S110-200%-45° CSP specimen. The faceted area extends to a depth of approximately 150 μm. The faceted area is surrounded by cleavage like fatigue fracture. **(d)** Crack initiation and crack growth of LSP 10GW/cm^2, 2 passes. The fractograph indicates surface crack initiation and crack branching at ~50 μm. The propagation path of Crack B is almost parallel to the direction of stress. **(e)** Crack initiation and early crack growth of LSP 10GW/cm^2, 3 passes. The fractograph indicates surface crack initiation and crack branching at ~90μm. The propagation path of crack A is almost parallel to the direction of stress. **(f)** Crack initiation and early crack growth of dual treatment. The fractograph indicates surface crack initiation from a typical shot-peening dent. Crack branching is also evident.

appears to have little effect on fatigue life. The poor performance of CSP is even more noticeable in the near 5 M cycles mark. To explain this performance, a theoretical analysis suggested in Ref. 9 is used. According to that work, part of the residual stress profile is used to counterbalance the increased roughening of the surface (amplified nominal stress). For the selected CSP treatment and the corresponding K_t, the analysis suggests a counterbalance residual stress between 90-125 MPa within the first 50 μm of depth for applied stress levels between 220 and 300 MPa. The above indicates that the remaining part of the residual stress profile should give some fatigue life increase.

2.2 Fractographic Analysis

To assist in the interpretation of the test data, an extensive fractographic analysis was performed. Fracture surfaces were examined using a Camscan Mark 2 SEM. Prior to examination, the surfaces were ultrasonically cleaned in an alcohol-based solution. Figure 6 shows the crack nucleation site and early crack growth of all six test groups at a maximum stress of 300 MPa.

The lack of surface stress concentration features in the specimen with the mirror-like finish leads to a single crack nucleus (possible at an inclusion) and to a surface crack of an almost semi-circular shape (Fig. 6a). On the other hand, the rough surface of the EDM finish promotes multiple crack nucleation sites, which join at an early stage, and the crack adopts an elongated semi-elliptical shape (Fig. 6b). The fracture surface of the 4A CSP shows limited faceted crack growth and extensive evidence of cleavage-like fatigue growth, which cannot be explained by the faster growing corner crack. The above reinforces the initial assumption of ductility loss. Ductility loss can be attributed to a very high and irregular dislocation density in the near surface region caused by work hardening. In the case of LSP, the fracture surfaces indicate branching of the crack. In both cases (2 passes or 3 passes), a part of the crack was observed to propagate almost parallel to the direction of the stress indicating slow crack growth rate. Close examination of the crack paths and the corresponding residual stress profiles indicates the tendency of the "parallel" crack to propagate along the minimum in the residual stress profile. On the other hand the "perpendicular" crack shows an extensive amount of faceted growth, especially in the case of 2 passes. The dual treatment shows evidence of fracture more similar to LSP (crack branching). In contrast to CSP, the dual treatment shows no evidence of cleavage-like fracture.

Considering that both the CSP and the dual treatment provided strain hardening of the near surface layer and also that only the CSP showed evidence of ductility loss, it is assumed that in the case of the dual treatment the residual stresses, created by the LSP, compensated for the possible ductility loss by possible rearrangement of the near surface dislocations. This could imply that the poor fatigue performance of the CSP material is possibly due to the partial relaxation of the residual stresses. Herein, it important to note that residual stress relaxation is time and stress level dependent. Thus, a better understanding could be obtained by relating the residual stress relaxation pattern to crack length.

3. Discussion and Conclusions

In this work, an extensive investigation was conducted to examine and compare different surface treatments and different surface finish conditions on the fatigue behavior of 2424-T351 aluminum alloy. The objectives of the investigation were (1) to examine the possible fatigue life improvement provided by different industrially available surface treatments and (2) to investigate possible reduction of the production cost by employing surface engineering on poorly surface finished components.

Fatigue data showed that even though all treatments (CSP, LSP and dual) improved fatigue life, the LSP and dual treatment had a far more superior performance. Fractographic analysis indicated that this was due to the phenomena of ductility loss and possible residual stress relaxation experienced by the CSP, and not by the LSP and dual treated specimens.

In summary, the following conclusions can be drawn:

- CSP, LSP, and dual treatments are expected to increase the fatigue life of poorly machined components and thus reducing the production cost.
- LSP was found to cause negligible strain hardening as in the case of CSP and dual treatment.
- LSP and dual treatments exhibit a far more superior fatigue improvement compared to CSP.
- Ductility loss due to strain hardening and possible residual stress relaxation is possible in CSP and requires further research.
- Pre-stressing the material (dual treatment) can increase the magnitude of the residual stress profile while at the same time stabilises the residual stresses.

Acknowledgement

The authors wish to express their gratitude to the EPSRC (UK), the Royal Academy of Engineering, CONACyT-ITTLA (Mexico), Airbus UK, A. Levers, and the technical staff of the Department of Mechanical Engineering-University of Sheffield and the Sorby Centre.

References

1. Anon: *Shot Peening Applications,* 7th ed., Metal Improvement Company Inc., Paramus, NJ, 1998.
2. O. Vöhringer: "Changes in the State of the Material by Shot Peening" in *Int. Conf. On Shot Peening 3,* H. Wohlfahrt, R. Kopp and O. Vöhringer, ed., 1987, pp. 185-204.
3. I. Altenberger and B. Scholtes: "Improvement of Fatigue Lifetime of Mechanically Surface Treated Materials in the Low Cycle Fatigue Regime" in *Surface Treatments IV,* C.A. Brebbia and J.M. Kenny, ed., WIT Press, Southampton, UK, 1999, pp. 281-90.
4. T. Dörr and L. Wagner: "Fatigue Response of Various Titanium Alloys to Shot Peening" in *Surface Treatments IV,* C.A. Brebbia and J. M. Kenny, ed., WIT Press, Southampton, UK, 1999, pp. 349-57.
5. R.N. Pangborn and S. Weissmann: "Prediction of Fatigue Life by X-Ray Diffraction Methods," *Fatig. Eng. Mater.,* 1979, *1,* pp. 363-69.
6. L. Wagner and G. Lütjering: "Influence of Shot Peening on the Fatigue Behaviour of Ti-Alloys" in *Shot Peening,* Pergamon Press, New York, NY, 1981, pp. 453-60.
7. W. Kaysser: "Surface Modifications in Aerospace Applications," *Surf. Eng.,* 2001, *17,* pp. 305-11.

8. P. Starker, H. Wohlfahrt, and E. Macherauch: "Subsurface Crack Initiation During Fatigue as a Result of Residual Stresses" *Fatig. Fract. Eng. Mater. Struct.*, 1979, *1,* pp. 319-27.
9. S. Curtis, E.R. de los Rios, C.A. Rodopoulos, and A. Levers: "Analysis of the Effects of Controlled Shot Peening on Fatigue Damage of High Strength Aluminum Alloys," *Int. J. Fatigue,* 2003, *25,* pp. 59-66.
10. Anon: *Metals Handbook,* 9th ed., H.E. Boyer and T.L. Gall, ed., American Society of Metals, Metals Park, OH, 1997.
11. W.D. Callister Jr: *Materials Science and Engineering—An Introduction,* 2nd ed., Wiley, New York, 1991.
12. J. Solis-Romero, E.R. de los Rios, A. Levers, and S. Karuppanan: "Toward the Optimization of the Shot Peening Process in Terms of Fatigue Resistance of the 2024-T351 and 7150-T651 Aluminum Alloys" in *Surface Treatment V: Computer Methods and Experimental Measurements for Surface Treatment Effects,* C.A. Brebbia, ed., WIT Press, Southampton, UK, 2001, pp. 343-55.